

# Applied Electron Spectroscopy For Chemical Analysis

HASSAN WINDAWI

FLOYD F. L. HO

# Applied Electron Spectroscopy For Chemical Analysis

**HASSAN WINDAWI**

*UOP Corporate Research Center  
UOP Inc.  
Des Plaines, Illinois*

**FLOYD F.-L. HO**

*Hercules Research Center  
Hercules Incorporated  
Wilmington, Delaware*



**A WILEY-INTERSCIENCE PUBLICATION**

**JOHN WILEY & SONS**

**New York / Chichester / Brisbane / Toronto / Singapore**

Copyright © 1982 by John Wiley & Sons, Inc.

All rights reserved. Published simultaneously in Canada.

Reproduction or translation of any part of this work beyond that permitted by Section 107 or 108 of the 1976 United States Copyright Act without the permission of the copyright owner is unlawful. Requests for permission or further information should be addressed to the Permissions Department, John Wiley & Sons, Inc.

**Library of Congress Cataloging in Publication Data**

Main entry under title:

Applied electron spectroscopy for chemical analysis.

(Chemical analysis, v. 63)

"A Wiley-Interscience publication."

Includes index.

1. Electron spectroscopy. I. Windawi, Hassan,  
1942- II. Ho, Floyd. III. Series.

QD96.E44A66 543'.085 82-4781

ISBN 0-471-09051-4 AACR2

Printed in the United States of America

10 9 8 7 6 5 4 3 2 1

## CONTRIBUTORS

Dennis S. Everhart  
Kenan Laboratories of Chemistry  
University of North Carolina  
Chapel Hill, North Carolina

David M. Hercules  
Department of Chemistry  
University of Pittsburgh  
Pittsburgh, Pennsylvania

Floyd F.-L. Ho  
Hercules Research Center  
Hercules Incorporated  
Wilmington, Delaware

L. L. Kazmerski  
Photovoltaics Research Branch  
Solar Energy Research Institute  
Golden, Colorado

Joseph C. Klein  
Department of Chemistry  
University of Pittsburgh  
Pittsburgh, Pennsylvania

G. E. McGuire  
Tektronix Incorporated  
P.O. Box 500  
Beaverton, Oregon

N. S. McIntyre  
Brookhaven National Laboratory  
Department of Nuclear Energy  
Bldg. 830  
Upton, New York

C. J. Powell  
Surface Science Division  
National Bureau of Standards  
Washington, D.C.

Charles N. Reilley  
Kenan Laboratories of Chemistry  
University of North Carolina  
Chapel Hill, North Carolina

J. H. Thomas, III  
RCA Laboratories  
Princeton, New Jersey

C. D. Wagner  
Surfex Company  
29 Starview Drive  
Oakland, California

H. Windawi  
UOP Corporate Research Center  
UOP Inc.  
Des Plaines, Illinois

## PREFACE

Surface phenomena, a very common and yet extremely complex subject, are with us in our daily life as well as in our scientific endeavors, such as investigations in adhesion, catalysis, corrosion, enzymatic reactions, and of various solid state surfaces and interfaces. These studies have benefited greatly from the recent development of various surface-sensitive techniques and instruments. Among these developments is electron spectroscopy for chemical analysis (ESCA), which is also commonly termed x-ray photoelectron spectroscopy (XPS). In addition to its surface sensitivity, ESCA is uniquely capable of providing chemical information such as oxidation state and chemical bonding, as well as elemental compositions. In conjunction with ion milling or chemical etching, it has the ability to furnish a depth profile of both a surface and subsurface. In the last few years, ESCA has rapidly become a useful tool for every scientist dealing with surface properties of various materials. In this regard, a symposium on the chemical application of ESCA was held at the seventh Federation of Analytical Chemistry and Spectroscopy Societies (FACSS) meeting in Philadelphia on October 2, 1980. This monograph is a direct result of this symposium, with most presentations revised and extended to cover pertinent references up to early 1981.

In addition to critical review of major developments, new and significant advances from the authors' own laboratories were described at the symposium. To put the technique of ESCA in proper perspective, the experimental method in ESCA was featured (G. E. McGuire) and compared with other surface-analysis techniques (C. J. Powell). The applications dealing with various surfaces and interfaces of metals and metal oxides, such as solid state devices (J. H. Thomas, III), photovoltaic cells (L. L. Kazmerski), and corrosion processes (N. S. McIntyre) were discussed. Measurement of functional groups on polymer films was highlighted (C. N. Reilly, D. S. Everhart, and F. F.-L. Ho), and development in characterization of polymer-anchored homogeneous catalysts was covered (F. F.-L. Ho). Special features of application in heterogeneous catalysis (D. M. Hercules and J. C. Klein), as well as techniques in dealing with heterogeneous materials in general (H. Windawi and C. D. Wagner), were presented.

It is the editors' particular pleasure to acknowledge herein the contributions and genuine efforts of the individual authors as well as those of the reviewers. The comments and patience of the Series Editors and the publication staff are highly appreciated. We are, nevertheless, grieved by the untimely death of

Professor Charles N. Reilly of the University of North Carolina on December 31, 1981. On a happier note we express our congratulations to K. Siegbahn for being awarded the Nobel prize for 1981, which was partly based on his pioneering work in ESCA.

## PREFACE

*Des Plaines, Illinois*

Hassan Windawi

*Wilmington, Delaware*

Floyd F.-L. Ho

*August 1982*

## CONTENTS

<b>Chapter 1. INSTRUMENTAL METHODS IN ESCA</b>	<b>1</b>
by <i>G. E. McGuire</i> , Tektronix Incorporated	
<b>Chapter 2. COMPARISON OF ESCA WITH OTHER SURFACE-ANALYSIS TECHNIQUES</b>	<b>19</b>
by <i>C. J. Powell</i> , National Bureau of Standards	
<b>Chapter 3. XPS ANALYSIS OF SOLID STATE ELECTRON DEVICE STRUCTURES</b>	<b>37</b>
by <i>J. H. Thomas III</i> , RCA Laboratories	
<b>Chapter 4. X-RAY PHOTOELECTRON SPECTROSCOPY APPLICATIONS IN PHOTOVOLTAICS RESEARCH</b>	<b>61</b>
by <i>L. L. Kazmerski</i> , Solar Energy Research Institute	
<b>Chapter 5. ANALYSIS OF CORROSION FILMS USING XPS: ADVANTAGES AND LIMITATIONS</b>	<b>89</b>
by <i>N. S. McIntyre</i> , Brookhaven National Laboratory	
<b>Chapter 6. ESCA ANALYSIS OF FUNCTIONAL GROUPS ON MODIFIED POLYMER SURFACES</b>	<b>105</b>
by <i>C. N. Reilley</i> and <i>D. S. Everhart</i> , University of North Carolina, and <i>F. F.-L. Ho</i> , Hercules Inc.	
<b>Chapter 7. CHARACTERIZATION OF POLYMER-ANCHORED HOMOGENEOUS CATALYSTS—AN ESCA APPLICATION</b>	<b>135</b>
by <i>F. F.-L. Ho</i> , Hercules Inc.	
<b>Chapter 8. ELECTRON SPECTROSCOPY FOR CHEMICAL ANALYSIS APPLIED TO HETEROGENEOUS CATALYSIS</b>	<b>147</b>
by <i>D. M. Hercules</i> and <i>J. C. Klein</i> , University of Pittsburgh	
<b>Chapter 9. USE OF ESCA IN THE CHARACTERIZATION OF HETEROGENEOUS MATERIALS</b>	<b>191</b>
by <i>H. Windawi</i> , UOP Inc., and <i>C. D. Wagner</i> , Surfex Company	
<b>Index</b>	<b>209</b>

## CHAPTER

1

# INSTRUMENTAL METHODS IN ESCA

G. E. McGUIRE

*Tektronix Incorporated  
Beaverton, Oregon*

1. Introduction	1
2. Fundamentals	2
3. Instrumentation	3
3.1. Energy Analyzers	3
3.2. Electron Detectors	5
3.3. Magnetic Shielding	6
3.4. Vacuum Systems	6
3.5. X-ray Source	7
3.6. X-ray Monochromator	9
3.7. Excitation Sources	10
4. Spectral Features	11
4.1. Data Presentation	11
4.2. Line Broadening	13
4.3. Chemical Effects	14
5. Conclusion	16
References	17

## 1. INTRODUCTION

Photoelectron spectroscopy is growing in popularity as a general analytical tool, specifically in the area of surface analysis. In essence, it involves the energy analysis of electrons ejected from matter by incident radiation. It allows the investigation of electronic structure, providing a picture of molecular orbitals for gas-phase species, valence band density of states, and core-level electron-binding energies for solids. The characteristic electron energies allow elemental analysis as well as chemical state identification. In addition, photoelectron spectroscopy probes only the surface region of solids. As a result, the technique is frequently used in investigations of phenomena such as absorption, corrosion, catalysis, adhesion, and segregation, where surface composition is of great importance.



The phenomenon of photoemission when a material is exposed to electromagnetic radiation of sufficient energy has been known for quite a long time. It was not until the late 1960s that significant developments in the field of photoelectron spectroscopy occurred that led to the current awareness of the technique. K. Siegbahn and others in the Physics Department of the University of Uppsala, Sweden, published pioneering works in the field in 1967<sup>1</sup> and 1969<sup>2</sup> which described in detail many aspects of electron spectroscopy as they are known today. In their 1967 study, Siegbahn et al. coined the term *electron spectroscopy for chemical analysis* (ESCA), which is now frequently used interchangeably with *x-ray excited photoelectron spectroscopy* (XPS). About the same time, D. W. Turner and his colleagues at the University of Oxford, England, published their work on *ultraviolet photoelectron spectroscopy* (UPS) of molecular gases.<sup>3</sup> Commercial instrumentation for XPS of solids and UPS of gases became available around 1970. Rapid development of the technique took place over the next few years resulting in a merging of the instrumentation for XPS and UPS. In 1972 a journal was founded that was devoted to the topic, namely, *Journal of Electron Spectroscopy and Related Phenomena*. Nowadays, it is difficult to find a chemical journal that does not contain some articles related to photoelectron spectroscopy. Interest in the application of this technique to surface analysis in a wide variety of fields has resulted in several international conferences<sup>4</sup> on the subject and volumes such as the present one.

## 2. FUNDAMENTALS

If a sample is irradiated with monochromatic photons of frequency  $\nu$ , the photons may be absorbed resulting in the emission of electrons defined by the Einstein relation,<sup>5</sup>

$$h\nu = E_{\text{BE}} + E_{\text{K}} \quad (1)$$

$E_{\text{BE}}$  is the ionization energy or binding energy of the  $k$ th species of electron in the material, and  $E_{\text{K}}$  is the kinetic energy of the ejected electron. A photoelectron ejected from a free molecule will have lower kinetic energy due to vibrational and rotational energy imparted to the molecule by the photon. For solids, the vibrational and rotational terms are usually neglected, although Citrin et al.<sup>6</sup> found core photoelectron transitions in alkali halides exhibit temperature-dependent line widths consistent with excitation of lattice vibrations during photoemission. Including correction terms for the spectrometer work function  $\phi_{\text{sp}}$  and sample charging  $\phi_{\text{sa}}$ , Equation 1 becomes

$$h\nu = E_{\text{BE}} + E_{\text{K}} + \phi_{\text{sp}} + \phi_{\text{sa}} \quad (2)$$

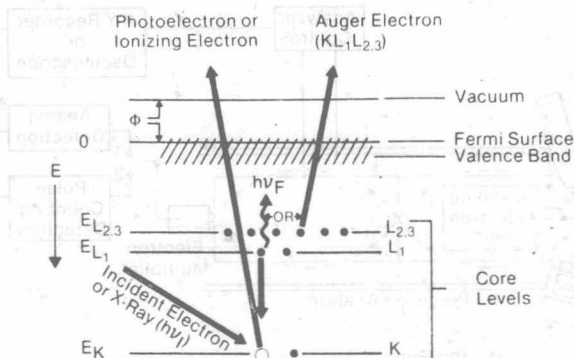


Figure 1. Energy level diagram of electron or photon excitation of an atom that results in photoionization and the subsequent relaxation that results in Auger electron or x-ray emission.

Assuming that the Fermi level of the sample and spectrometer align, the binding energy of any core level, as shown in Figure 1, is the energy separation between that core level and the Fermi level of the sample. For conductive samples in contact with an electron spectrometer, the Fermi levels of the sample and spectrometer will be coincident. As a result, the spectrometer work function can be determined by obtaining the spectrum of a conductive material with known binding energies. The instrument is adjusted until the binding energies agree with the known value. The spectrometer work function remains relatively constant. When the apparatus has been exposed to atmospheric pressure for maintenance or other purposes, a redetermination of  $\phi_{sp}$  may be necessary.

For semiconductors and insulators the Fermi level lies somewhere between the filled valence band and empty conduction band. The Fermi level for semiconductors and insulators is obtained by determining the specimen work function using internal calibration or charge correction.<sup>7</sup> Internal calibration is accomplished by mixing or evaporating a conductive material with known binding energies onto the sample.

### 3. INSTRUMENTATION

#### 3.1. Energy Analyzers

The kinetic energy of the ejected electron is measured using an electrostatic or magnetic analyzer. The function of the energy analyzer is to measure the number of photoelectrons as a function of their energy. Of all the analyzer designs, the double-pass cylindrical mirror and 180° spherical sector analyzer are among the

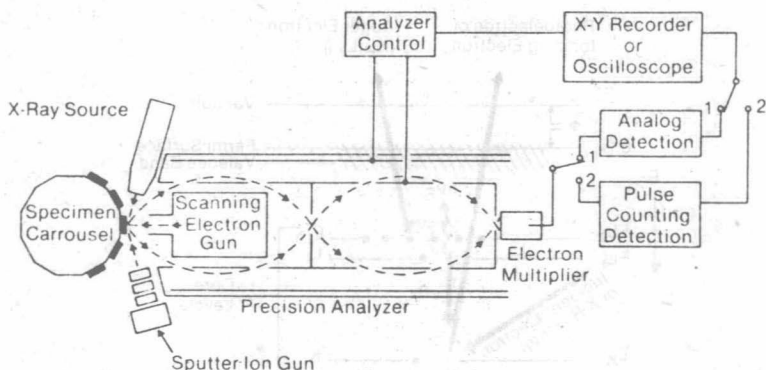


Figure 2. The geometry of a double-pass cylindrical mirror analyzer used for x-ray photoelectron spectroscopy.

most popular in commercial instrumentation. Figure 2 shows a schematic diagram of the double-pass cylindrical mirror analyzer. The analyzer consists of two stages of coaxial cylinders with a negative potential applied to the outer cylinder. The potential applied between the inner and outer cylinders creates a cylindrical retarding potential.<sup>8</sup> Electrons which leave the sample positioned at the focal point of the analyzer pass through an annular defining slit, then pass into the radial field between the cylinders to be focused back to the axis by the negative potential. The electrons pass into the second cylindrical mirror analyzer to be focused onto an electron multiplier.

The use of tandem cylindrical capacitors improves energy resolution over a single-stage device. Energy resolution is also improved by first decelerating the electrons through the use of a retarding field formed by spherical grids at the entrance to the analyzer. If electrons leaving the sample with kinetic energy  $E_K$  are retarded to an energy  $E_0$  for transmission through the analyzer, then the resolving power of the complete system will be improved by a factor equal to the retarding ratio,  $E_K/E_0$ . Retardation also gives rise to an improvement in sensitivity at a fixed energy resolution since a larger slit may be used at the lower transmission energies.

Retardation has been accomplished through the use of an electrostatic lens in conjunction with the  $180^\circ$  hemispherical analyzer shown schematically in Figure 3. The use of a lens focuses the electrons toward the acceptance angle of the analyzer. The use of an extracting and retarding lens also allows more variation in sample position due to its depth of focus. The hemispherical analyzer deflects the electrons  $180^\circ$  in the field between two concentric spheres. Electrons enter the analyzer near the center of the gap defined by a slit and exit after  $180^\circ$  deflection. Energy resolution is controlled by the radial source width, the axial

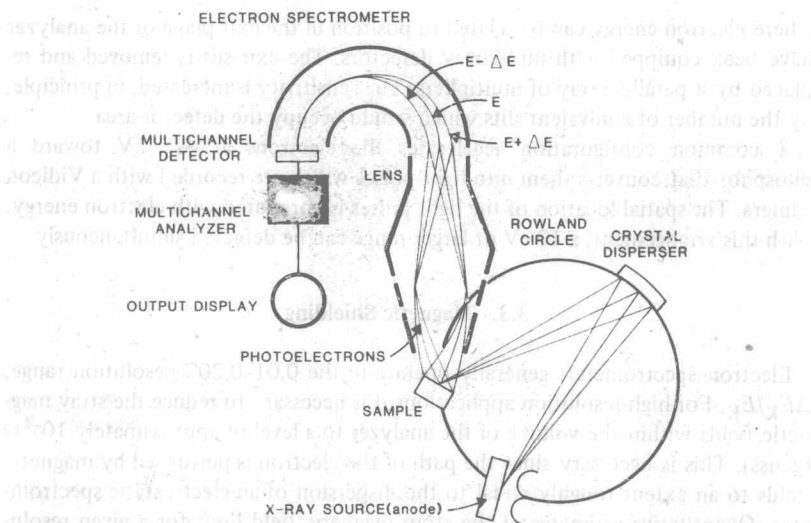


Figure 3. Schematic diagram of a 180° hemispherical analyzer with electrostatic lens.

source height, the detector width, the radial angle of emission, the axial angle of emission, and the optic circle radius.<sup>9</sup>

It is necessary to terminate the fringing fields at the entrance and exit to the electrodes of both the cylindrical (CMA) and hemispherical analyzers. Fringing fields at the ends of the CMA may be terminated by a series of rings coupled by dividing resistors or by resistively coated ceramic disks. The fringing fields of the hemispherical analyzer may be terminated by concentric wires or shaped electrodes biased at the electron pass energy.

### 3.2. Electron Detectors

The most commonly used detectors in XPS are channel electron multipliers.<sup>10</sup> These consist of lead-doped glass tubes with a semiconducting coating possessing a high secondary electron yield. A high voltage of a few kilovolts is applied between the ends of the multiplier to produce a gain of  $10^6$ – $10^8$  due to the cascade of collisions as electrons travel down the inside of the tube. The detectors are frequently coiled to reduce noise due to ions produced in the multiplier. They have a high gain even for electrons at low kinetic energy and a low background count of less than 1 count per minute. The output of the multiplier is a series of pulses that are fed into a pulse amplifier-discriminator, then into a digital-to-analog converter, and stored in a multichannel analyzer or a computer.

Spherical and cylindrical sector spectrometers with a well-defined focal plane

where electron energy can be related to position in the exit plane of the analyzer have been equipped with multiarray detectors. The exit slit is removed and replaced by a parallel array of multipliers. The sensitivity is increased, in principle, by the number of equivalent slits which would occupy the detector area.

A common configuration accelerates the electrons at 4-5 kV toward a phosphor that converts them into light pulses which are recorded with a Vidicon camera. The spatial location of the light pulses is correlated with electron energy. With this arrangement, a 10 eV or larger range can be detected simultaneously.

### 3.3. Magnetic Shielding

Electron spectrometers generally operate in the 0.01-0.20% resolution range,  $\Delta E_K/E_K$ . For high-resolution applications it is necessary to reduce the stray magnetic fields within the volume of the analyzer to a level of approximately  $10^{-4}$  G (gauss). This is necessary since the path of the electron is perturbed by magnetic fields to an extent roughly equal to the dispersion of an electrostatic spectrometer. Quantitative estimates of the stray magnetic field limit for a given resolution may be calculated.<sup>11</sup> Magnetic field cancellation has been accomplished by using sets of Helmholtz coils<sup>12</sup> or ferromagnetic shielding.<sup>13</sup> Ferromagnetic shielding is used exclusively on commercial spectrometers because it is simple, compact, and less sensitive to magnetic field variations. Caution should be exercised since localized areas of magnetism can develop due to accidental blows to the shielding or by contact with strong magnetic fields. Degaussing with an RF (radio-frequency) coil after any activity that requires entering the analyzer housing is a common safety precaution. Shielding is accomplished by using two or more layers of commercially available ferromagnetic alloys (i.e., conetic or mu-metal) whose permeability ratio is several orders of magnitude greater than iron.

### 3.4. Vacuum Systems

The vacuum system that is used must maintain a pressure so that photoelectrons have a long mean free path relative to the dimensions of the spectrometer and so that the partial pressure of residual gases will not contaminate the sample surface during the time of analysis. The requirement for a long electron mean free path is satisfied at pressures at  $10^{-3}$  Pa or lower. The surface sensitivity of XPS requires total pressures of  $\leq 10^{-7}$  Pa in order to permit adequate control of surface composition. The time to build up a monolayer of residual gas will depend on the pressure and the sticking coefficient of the gas. Adequate pressures can be achieved by a variety of techniques<sup>14</sup>; however, the most common system is a getter-ion pump complemented by a sublimation pump with a cryogenic shroud and sorption forepump. The vacuum system is of stainless steel

construction with crushed metal gaskets. Using this approach, total pressures of  $10^{-9}$  Pa can be achieved.

### 3.5. X-ray Source

Figure 2 shows the x-ray excitation source positioned in proximity to the sample and to the entrance to the analyzer to ensure the greatest solid angle between the x-ray anode and the sample and between the sample and the analyzer. The basic x-ray source includes a heated filament and a large target anode. Electrons from the filament are accelerated toward the anode to produce radiation that consists of a continuum of bremsstrahlung radiation with characteristic x-ray lines superimposed upon it. The continuum has a maximum energy that corresponds to the maximum energy of the bombarding electrons and a maximum intensity between one-half and two-thirds of the primary electron energy. The characteristic x-ray lines are a result of relaxation of atoms ionized during electron bombardment. During the relaxation process, electrons from an outer shell fill inner shell vacancies while simultaneously emitting an x-ray.

X-ray sources are constructed in a variety of ways. Figure 4 shows the basic

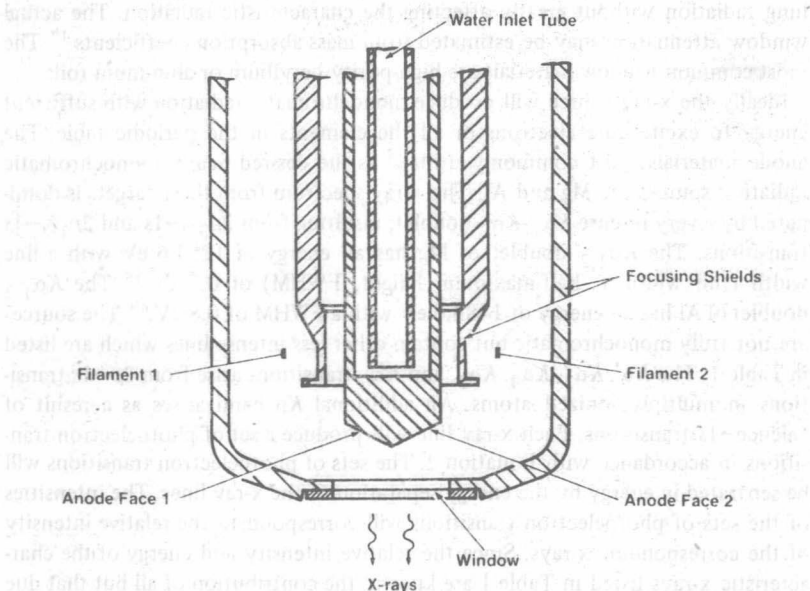


Figure 4. X-ray source with dual filament and anode faces capable of separate x-ray excitation. (After A. Barrie, in *Handbook of X-ray and Ultraviolet Photoelectron Spectroscopy*, D. Briggs, Ed., Heyden, London, 1977, p. 83.

components of a dual anode x-ray source, which are basically the same as those of a single anode source. The anode is held at a high positive potential while the filament is held near ground potential.<sup>15</sup> The positive potential on the anode ensures that scattered electrons do not enter the sample chamber but are reattracted to the anode. The cooling water source that dissipates heat from the tip of the anode must be electrically isolated when the anode is operated at positive potential. The filaments are positioned out of line of sight of the anode to prevent the deposition of filament material on the anode target. Buildup of contamination on the target would significantly attenuate the number of x-rays emitted from the source. Independent operation of either filament can selectively excite either anode face.

The efficiency of x-ray production is only about one percent of the total applied power.<sup>16</sup> The actual intensity of x-rays produced depends on the voltage and current of the electron beam striking the anode. The threshold energy for the process is the binding energy of the inner shell electrons. The intensity of x-ray production just above threshold is very low but increases rapidly to a maximum some 5-10 times the threshold energy.

A thin, x-ray transmitting window separates the excitation region from the specimen. The window prevents the entry of scattered electrons from the x-ray source into the sample chamber. It also must attenuate high-energy bremsstrahlung radiation without greatly affecting the characteristic radiation. The actual window attenuation may be estimated from mass absorption coefficients.<sup>17</sup> The most common window materials are high-purity beryllium or aluminum foils.

Ideally the x-ray source will produce monochromatic radiation with sufficient energy to excite core electrons of all the elements in the periodic table. The anode materials most commonly utilized as the desired nearly monochromatic radiation sources are Mg and Al. The x-ray spectrum from these targets is dominated by a very intense  $K\alpha_1$ - $K\alpha_2$  doublet, resulting from  $2p_{3/2} \rightarrow 1s$  and  $2p_{1/2} \rightarrow 1s$  transitions. The  $K\alpha_{1,2}$  doublet of Mg has an energy of 1253.6 eV with a line width (full width at half-maximum height, FWHM) of 0.7 eV.<sup>18</sup> The  $K\alpha_{1,2}$  doublet of Al has an energy of 1486.6 eV with a FWHM of 0.8 eV.<sup>19</sup> The sources are not truly monochromatic but contain other less intense lines which are listed in Table 1. The  $K\alpha'$ ,  $K\alpha_3$ ,  $K\alpha_4$ ,  $K\alpha_5$ , and  $K\alpha_6$  transitions arise from  $2p \rightarrow 1s$  transitions in multiply ionized atoms. An additional  $K\beta$  band arises as a result of valence  $\rightarrow 1s$  transitions. Each x-ray line will produce a set of photoelectron transitions in accordance with Equation 2. The sets of photoelectron transitions will be separated in energy by the energy separation of the x-ray lines. The intensities of the sets of photoelectron transitions will correspond to the relative intensity of the corresponding x-rays. Since the relative intensity and energy of the characteristic x-rays listed in Table 1 are known, the contribution of all but that due to the  $AlK\alpha_{1,2}$  doublet may be subtracted from the XPS spectrum through suitable software.



TABLE 1. Characteristic X-rays Produced from Al and Mg Sources<sup>a</sup>

X-ray	Mg			Al		
	Energy (eV)	Relative intensity		Energy (eV)	Relative intensity	
K $\alpha_1$	1253.7	67	100.0	1486.7	67	100.0
K $\alpha_2$	1253.4	33		1486.3	33	
K $\alpha$	1258.2	1.0		1492.3	1.0	
K $\alpha_3$	1262.1	9.2		1496.3	7.8	
K $\alpha_4$	1263.7	5.1		1498.2	3.3	
K $\alpha_5$	1271.0	0.8		1506.5	0.42	
K $\alpha_6$	1274.2	0.5		1510.1	0.28	
K $\beta$	1302.0	2.0		1557.0	2.0	

<sup>a</sup>From M. O. Krause and J. G. Ferreira, *J. Phys.*, B8, 2007 (1975).

### 3.6. X-ray Monochromator

Another means of removing background produced by bremsstrahlung radiation and satellite peaks produced by the less intense characteristic x-ray transitions is through the use of an x-ray monochromator. X-ray monochromators for specific application to XPS have been constructed using the 10 $\bar{1}0$  planes of quartz to diffract AlK $\alpha$  radiation.<sup>20</sup> The first-order diffraction angle, according to the Bragg relation  $n\lambda = 2d \sin \theta$  is 78.5° when AlK $\alpha$  x-rays of  $\lambda = 8.3$  Å are diffracted off the 10 $\bar{1}0$  planes of quartz with  $2d = 8.5$  Å. Unwanted radiation is suppressed, while the ultimate resolution is improved by selecting a narrow band of the AlK $\alpha_{1,2}$  radiation through the use of the quartz monochromator. The theoretical limit is 0.16 eV<sup>20</sup> while the best actual resolution was 0.22 eV.<sup>21</sup> A more typical value for commercial instrumentation of 0.4 eV.<sup>22</sup>

Since only a small fraction of the incident radiation is reflected to the sample in crystal diffraction, the crystals are elastically bent or ground to the circumference of a Rowland circle. Bending focuses the x-rays to produce a high flux per unit area. More than one crystal can be used to increase the x-ray intensity if they are toroidally bent and arranged in the nondispersive plane of the Rowland circle.

The dispersion of a quartz crystal depends on the diameter of the Rowland circle and the finite width of the x-ray source. If a sharply focused electron beam is used to bombard the x-ray anode, a narrow x-ray energy spread will be focused on the Rowland circle. As the source size increases, the energy spread increases and is spatially distributed across the sample. The analyzer can be designed so that its dispersion is opposite but equal in magnitude to that of the monochromator.<sup>23</sup> In dispersion compensation the sample must be positioned at



the Rowland circle, while in fine focusing rough or irregular surfaces can be examined without loss of resolution. Since a larger source size can dissipate more heat, it can be operated at higher power than can a fine focusing source. In order to dissipate more heat from a fine focusing source, rotating anodes have been developed that effectively multiply the anode area by the circumference of the circular anode.

### 3.7. Excitation Sources

For nonmonochromatized x-ray sources, the primary limitation of instrumental resolution is the natural line width of the radiation. Table 2 lists a variety of sources that have been investigated<sup>13</sup>; however, the most frequently used remain Al and Mg. Narrower sources are available since the FWHM decreases with decreasing atomic number as a result of a decrease in spin-orbit splitting or an increase in the lifetime of the hole. Although materials of lower atomic number have more favorable FWHM, they are not used because of their chemical reactivity, poor thermal conductivity, or high vapor pressure. Table 2 also lists anode materials with x-ray energies higher than Al. Use of these materials results in loss of resolution in an XPS spectrum. More information is gained when one of the higher energy sources is used because of the excitation of more tightly bound Auger electrons and photoelectrons. When more than one source is available, as in the case of a dual anode source, higher energy x-rays may be used to complement Mg or Al.

When only one source is available, Mg or Al offer the best combination of excitation, energy, and resolution. Even then, high energy Auger lines may be excited by bremsstrahlung radiation in the normal operation of an x-ray anode.<sup>24</sup>

TABLE 2. X-ray Photoelectron Excitation Sources

Radiation	Energy (eV)	Full width at half-maximum height (eV)
Y $M\zeta$	132.3	0.44
Zr $M\zeta$	151.4	0.77
Na $K\alpha$	1041.0	0.4
Mg $K\alpha$	1253.6	0.7
Al $K\alpha$	1486.6	0.8
Si $K\alpha$	1739.4	0.8
Ti $K\alpha_1$	4511	1.4
Cr $K\alpha_1$	5415	2.1
Cu $K\alpha_1$	8048	2.5